

Supporting Information

Extrinsically 2D-Chiral Metamirror in Near-Infrared Region

Libang Mao,[†] Kuan Liu,[†] Shuang Zhang,[‡] and Tun Cao^{*,†}

[†]School of Optoelectronic Engineering and Instrumentation Science, Dalian

University of Technology, Dalian 116024, P. R. China

[‡]School of Physics & Astronomy, University of Birmingham, Birmingham, B15 2TT, UK

The number of pages: 5

The number of figures: 6

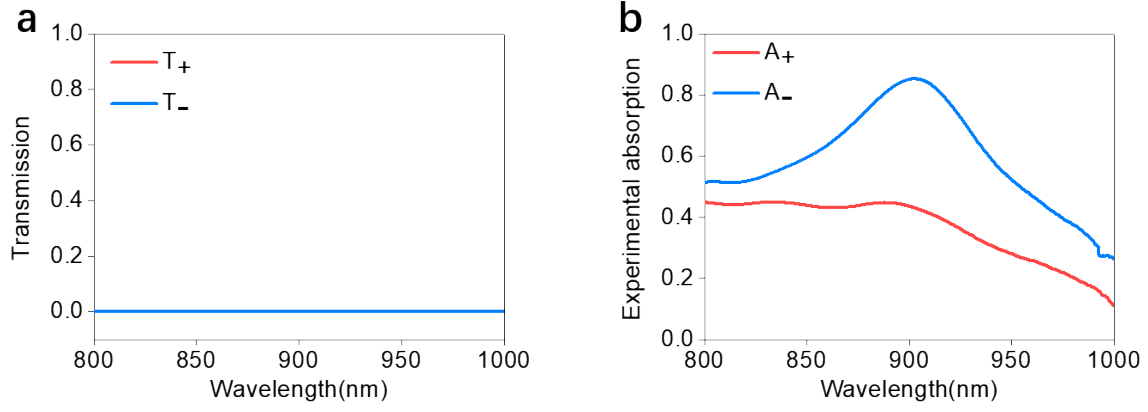


Figure S1. The measured (a) transmittance T_- , T_+ and (b) absorptance A_- , A_+ of the extrinsically 2D-chiral metamirror under both LCP and RCP incidences with $\theta_i = 45^\circ$ and $\varphi = 70^\circ$.

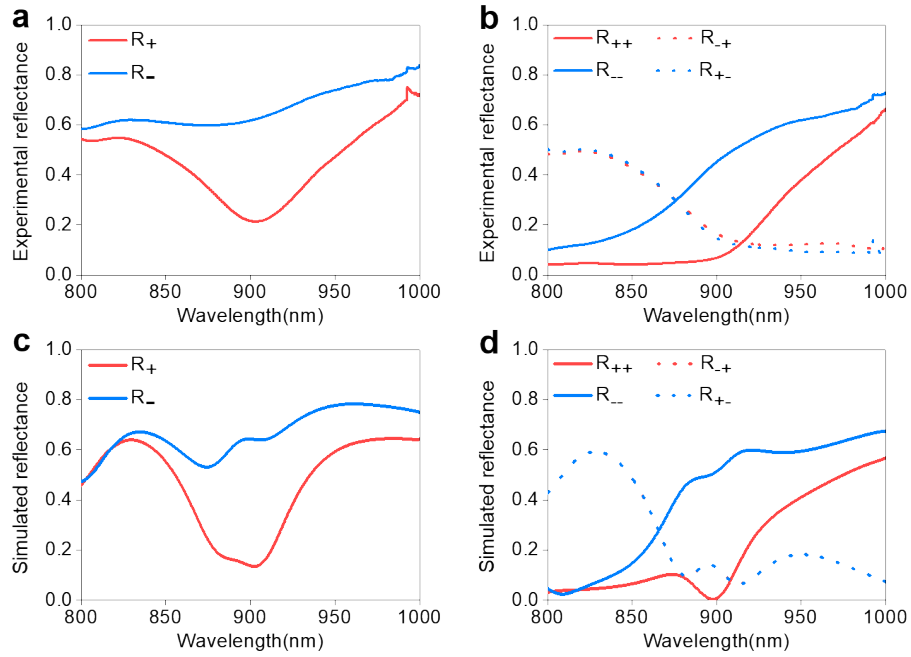


Figure S2. Simulated and measured reflectance of the extrinsically 2D-chiral metamirror. The measured reflectance spectra of (a) R_+ and R_- , (b) R_{++} , R_{--} , R_{+-} , and R_{-+} under both LCP and RCP incidences with $\theta_i = 45^\circ$ and $\varphi = -70^\circ$. The simulated reflectance spectra of (c) R_+ and R_- , (d) R_{++} , R_{--} , R_{+-} , and R_{-+} under both LCP and RCP incidences with $\theta_i = 45^\circ$ and $\varphi = -70^\circ$.

For grazing angle incidence, the higher diffraction orders appear when the periodicity is larger than half the wavelength, while for normal incident angle, this occurs when the period is larger than the wavelength. As our incident angle is somewhere in-between, the diffraction orders appear at a ratio between the period and wavelength somewhere between 0.5 and 1. More detailed analysis is given below:

It is known that the high-order diffraction is excited in the grating structure at $\lambda = \frac{2\pi}{\left| \vec{k}_{n,m} \right|}$,

where n, m represent the diffraction order along the x- and y- direction. The wavevector of the diffraction wave can be expressed by [51,52],

$$\left| \vec{k}_{n,m} \right| = \sqrt{\left| (\vec{k}_{n,m})_x \right|^2 + \left| (\vec{k}_{n,m})_y \right|^2 + \left| (\vec{k}_{n,m})_z \right|^2} \quad (1)$$

In our proposed metamirror, we can obtain

$$\left| (\vec{k}_{n,m})_x \right| = \left| (\vec{k}_{in})_x \right| + n \frac{2\pi}{P_x} \quad (2)$$

$$\left| (\vec{k}_{n,m})_y \right| = \left| (\vec{k}_{in})_y \right| + m \frac{2\pi}{P_y} \quad (3)$$

where \vec{k}_{in} is the wavevector of the incident light, $P_x = 760$ nm and $P_y = 420$ nm are the grating periods along the x- and y- directions, respectively. In this work, the $(\vec{k}_{in})_x$ and $(\vec{k}_{in})_y$ are associated with the incident angel of θ_i and rotation angle of φ , which is shown by

$$\left| (\vec{k}_{in})_x \right| = \left| \vec{k}_{in} \right| \cdot \sin \theta_i \cdot \cos \varphi \quad (4)$$

$$\left| (\vec{k}_{in})_y \right| = \left| \vec{k}_{in} \right| \cdot \sin \theta_i \cdot \sin \varphi \quad (5)$$

By placing equations (2-5) to equation (1), we have

$$\lambda = \frac{2\pi}{\sqrt{\left(\frac{2\pi}{\lambda} \cdot \sin \theta_i \cdot \cos \varphi + n \frac{2\pi}{P_x} \right)^2 + \left(\frac{2\pi}{\lambda} \cdot \sin \theta_i \cdot \sin \varphi + m \frac{2\pi}{P_y} \right)^2 + \left| (\vec{k}_{n,m})_z \right|^2}} \quad (6)$$

We thus obtain

$$\left| (\vec{k}_{n,m})_z \right|^2 = \frac{4\pi^2}{\lambda^2} - \left(\frac{2\pi}{\lambda} \cdot \sin \theta_i \cdot \cos \varphi + n \frac{2\pi}{P_x} \right)^2 - \left(\frac{2\pi}{\lambda} \cdot \sin \theta_i \cdot \sin \varphi + m \frac{2\pi}{P_y} \right)^2 \geq 0 \quad (7)$$

For the $(n, m) = (-1, 0)$ order diffracted beam, we have

$$\lambda \leq P_x \cdot \left(\sqrt{1 - (\sin \theta_i \cdot \sin \varphi)^2} + \sin \theta_i \cdot \cos \varphi \right) \quad (8)$$

For the $(+1, 0)$ order,

$$\lambda \leq P_x \cdot \left(\sqrt{1 - (\sin \theta_i \cdot \sin \varphi)^2} - \sin \theta_i \cdot \cos \varphi \right) \quad (9)$$

For $(0, -1)$ order,

$$\lambda \leq P_y \cdot \left(\sqrt{1 - (\sin \theta_i \cdot \sin \varphi)^2} + \sin \theta_i \cdot \cos \varphi \right) \quad (10)$$

For $(0, +1)$ order,

$$\lambda \leq P_y \cdot \left(\sqrt{1 - (\sin \theta_i \cdot \sin \varphi)^2} - \sin \theta_i \cdot \cos \varphi \right) \quad (11)$$

By placing $P_x = 760$ nm, $P_y = 420$ nm, $\theta_i = 45^\circ$, $\varphi = 70^\circ$ to Eqs.(8)-(11), we get $\lambda \leq 750, 384, 415$, and 212 nm for $(-1, 0)$, $(+1, 0)$, $(0, -1)$, and $(0, +1)$ order diffracted beam, respectively. It means that the higher order diffracted beams would appear when the incident wavelength is smaller than 750 nm. To avoid the influence of the high-order diffraction, we set the incident wavelength at $\lambda = 910$ nm. Therefore, in our case the higher order diffracted beams are not excited.

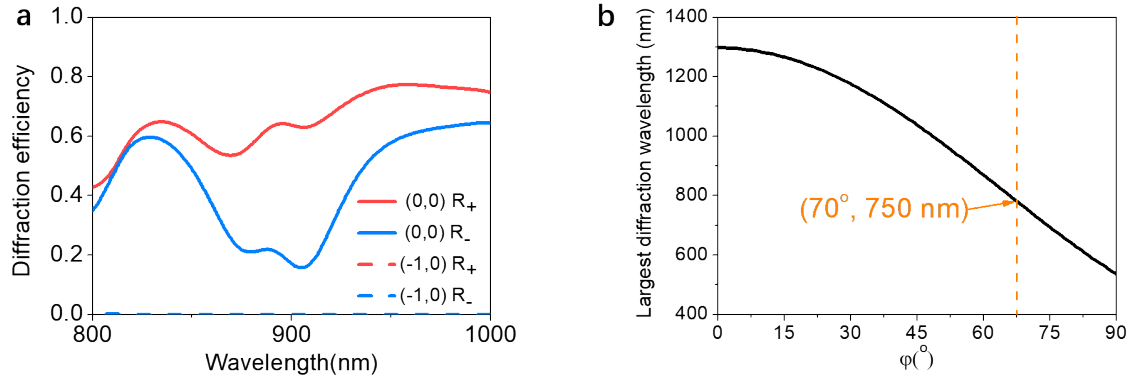


Figure S3. (a) Simulated diffraction efficiency of the 2D-chiral metamirror for different diffraction orders under both LCP and RCP incidences with $\theta_i = 45^\circ$ and $\varphi = 70^\circ$. (b) The largest wavelength for which the $(-1, 0)$ high-order diffraction occurs as varying the φ from 0 to 90° while fixing $\theta_i = 45^\circ$.

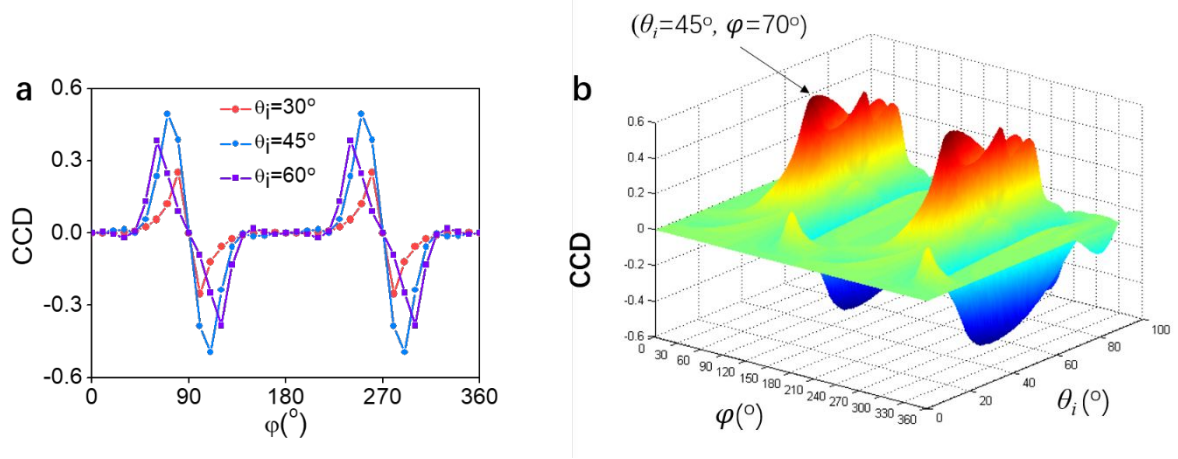


Figure S4. (a) The simulated ϕ dependent CCD signal with $\theta_i = 30^\circ$, 45° , and 60° at $\lambda = 910$ nm. (b) 2D diagram of CCD against θ_i and ϕ at $\lambda = 910$ nm.

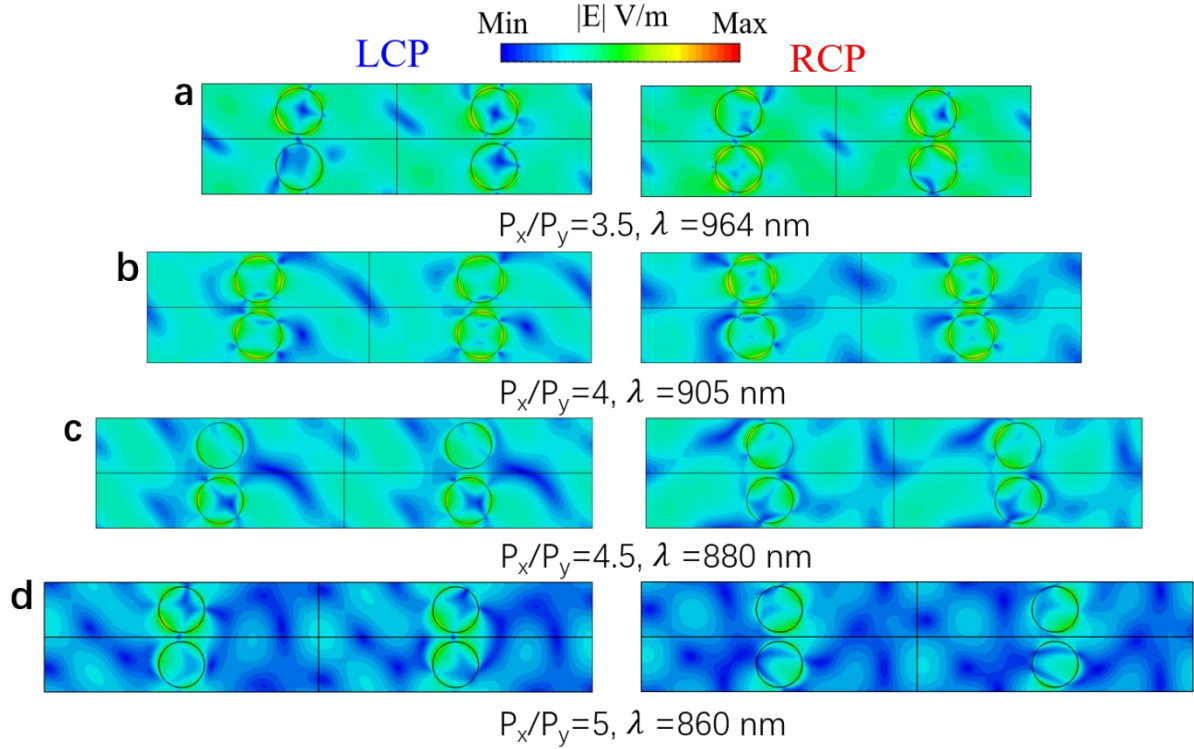


Figure S5. The normalised E - field distributions at the air-metamirror interface under the oblique CPL incidences with $\theta_i = 45^\circ$ and $\phi = 70^\circ$ for (a) $P_x/P_y = 3.5$, $\lambda = 964$ nm, (b) $P_x/P_y = 4$, $\lambda = 905$ nm, (c) $P_x/P_y = 4.5$, $\lambda = 880$ nm, (d) $P_x/P_y = 5$, $\lambda = 860$ nm. The response to LCP and RCP incidence is shown on the left and right, respectively.

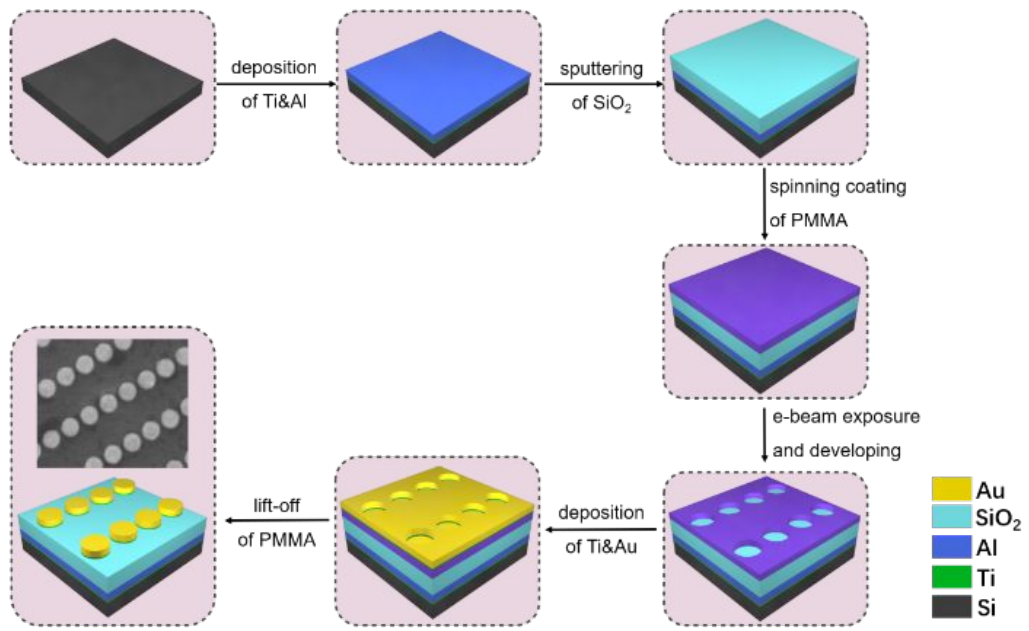


Figure S6. The schematic of fabrication processing of the metamirror.